Stress Distribution in Mandible Regulated by Bone and Dental Implant Parameters: Part I - Methodology

R. C. van Staden[1], H. Guan[1], Y. C. Loo[1], N. W. Johnson[2], N. Meredith[3]
[1]*Griffith School of Engineering, Griffith University Gold Coast Campus, Australia*
[2]*School of Dentistry and Oral Health, Griffith University Gold Coast Campus, Australia*
[3]*Neoss Ltd, Harrogate, United Kingdom*

Abstract: The complicated inter-relationships between mandibular bone components and dental implants have attracted the attention of many a structural mechanics researcher as well as many a dental practitioner. This paper describes the methodology and analysis techniques employed to enable accurate evaluation of a vast range of the implant and bone parameters. The complex material and geometric properties of the bone and implant are modelled using two-dimensional (2D) triangular and quadrilateral plane strain elements. Assumptions made in the analysis include: (a) 50% osseointegration between bone and implant; (b) linear relationships exist between the stress value and the Young's moduli of the cancellous and cortical bone at any specific point. In the companion paper (Part II) various bone, implant and loading parameters are evaluated for their influence on the stress distribution within the bone, in particular in the mandible.

Keywords: bone, implant and loading parameters, finite element technique.

1 Introduction

Dental implants are biocompatible screw-like titanium 'fixtures' that are surgically placed into the jawbone to replace missing teeth. The mechanism by which an implant is bio-mechanically accepted by the jawbone is called osseointegration [1,2]. Stimulus of the bone through applied stresses has been well documented to influence the success or failure of an implant [3,4]. An optimum stress profile is required in order to maintain a strong and healthy jawbone: a stress that is too high may cause irreversible damage to the jawbone; one that is too low may fail to stimulate the jawbone sufficiently for satisfactory healing of the wound and thus, for osseointegration. Furthermore, the primary stability is especially critical because the bone is still in a state of repair and necessitates applied stresses that promote bone growth. Research by Himmlova et al. [5], Plikçiolu et al. [6] and Pierrisnard et al. [7] have all recognised the fact that the implant dimensions influence the magnitude and profile of stresses within the bone. It is commonly understood that increasing the implant length and/or diameter reduces the stresses within the bone. Furthermore, based on clinical experience practitioners appreciate the fact that if the bone is weak then a wider implant is required. However, these decisions are based primarily on clinical judgement but not supported by any theoretical data. It is critical for the practitioner to fully grasp the relationship between various combinations of bone, implant and loading parameters and the resulting stresses in the bone.

2 Modelling of Implant-Bone System

Modelling and simulation are performed using the Strand7 Finite Element Analysis System [8]. The first step of the modelling is to define the bone and implant geometry. This is then followed by specifying the material behaviour in terms of the Young's modulus, Poisson's ratio and density for various mandibular bone components and the implant. After applying the appropriate loading and restraint conditions, the various parameters and their contributions to the stress profile within the bone, in particular in the mandible, can be evaluated.

A 2D representation of the bone and implant is analysed because this is considered to be similarly accurate and more efficient in terms of computation time, as compared to a three dimensional equivalent. Data acquisition for the bone dimensions are carried out using Computed Tomography scanned images. The different types of bone, i.e. cancellous and cortical, are distinguished and the boundaries are identified in order to assign different material properties within the finite element model. Figure 1 shows a mandible section and implant with the loading and restraint conditions. Also shown in the figure are the detailed parameters considered in this study. The implant is cylindrical with 2 degrees of taperage and has a helical thread. For a particular finite element model with D = 4.5mm, L = 11mm, $Tcor$ = 1.2mm, the total numbers of elements are respectively 2870 for the implant, 5956 for cancellous bone, and 1094 and for cortical bone. The total number of nodal points in the entire model is 9969.

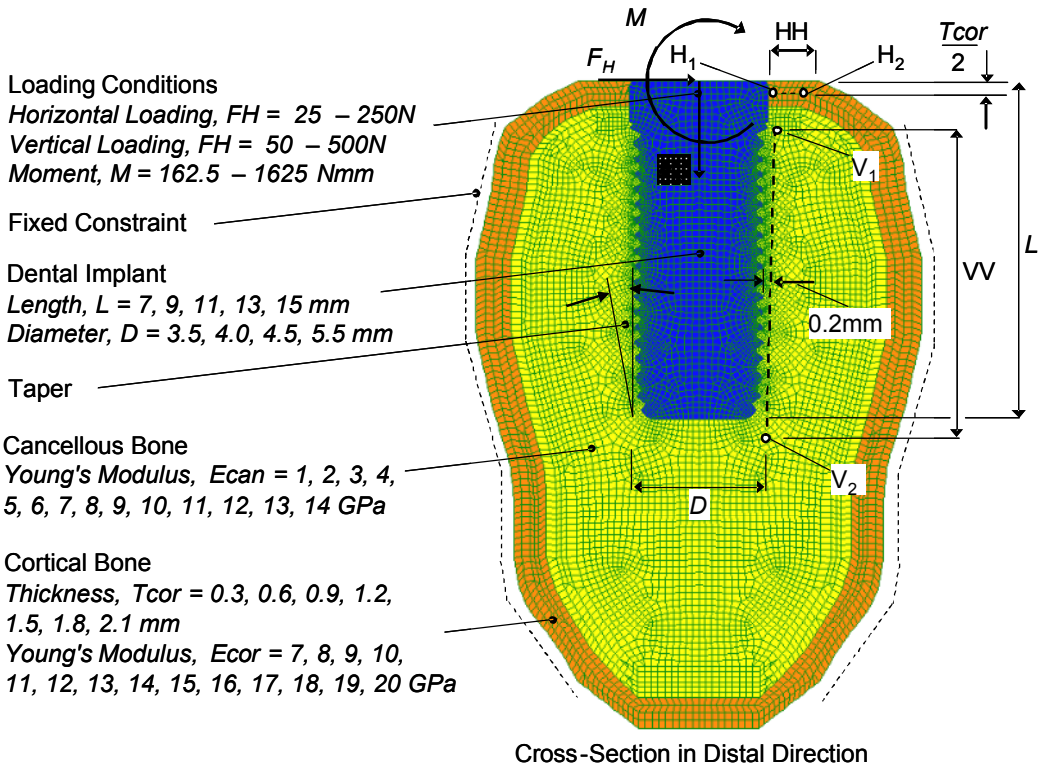

Figure 1: Finite element model of the mandible and dental implant

As indicated in Figure 1, the von Mises stresses along the lines VV for cancellous bone and HH for cortical bone are recorded for all possible parameter combinations. The stress characteristics along these two lines are believed to be critical in evaluating the performance of implantation [9]. Note that both lines VV and HH are chosen on the right side of the implant because the highest stress magnitudes occur on the right. This is due to the loading characteristics. The start and finish points of VV (i.e. V_1 and V_2) and HH (i.e. H_1 and H_2) are also identified in Figure 1 for ease of discussion.

A cross-sectional slice is taken from the mandible (refer to Figure 2). The "arc length" of the mandible is comparable to the width and depth of the slice. When the slice is subjected to in plane (x-y) masticatory forces (F_H, F_V and M), it is restrained from deforming out-of-plane (in the z-axis). Therefore, it can be assumed that all the strains are confined in the z-axis. To accurately represent the mechanical behaviour of the bone and implant, 3-node triangular (Tri3) and 4-node quadrilateral (Quad4) plane strain elements are therefore used for the construction of the finite element models. Note that for the plane strain elements each node has a complete set of spatial degrees of freedom including u and v. This means that each node can only translate in the x- (u) and y- (v) directions.

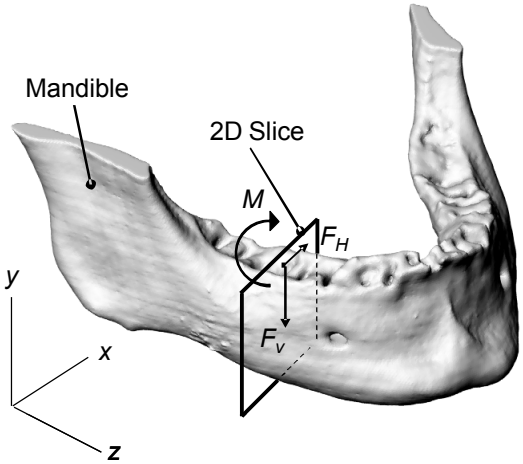

Figure 2: Location of 2D slice in a mandible

3 Parameters

3.1 Jaw bone

An extensive literature review by van Staden et al. [10] indicated that the commonly assumed range of Young's modulus values for cancellous bone is between 0.08 and 7.93GPa. For cortical bone it is normally assumed to vary from 5.57 to 22.8GPa. The present study adopts a range of Young's modulus for cancellous bone (*Ecan*) from 1 to 14GPa and for cortical bone (*Ecor*) from 7 to 20GPa, as summarised in Figure 1. The selection of such a range is based on the understanding that in some exceptional cases the Young's modulus of cancellous bone can go up to 14GPa when that of cortical bone is also at a high range. Assuming 1GPa intervals for these parameters results in fourteen different Young's modulus values for cancellous and cortical bone respectively. With such a large range of material parameters to be considered, the corresponding densities of cancellous and cortical bone must be determined. Equations 1 and 2 show the mean relationships between the Young's modulus and the density of cancellous (ρ_{can}) and cortical (ρ_{cor}) bone, respectively based on published works by Abendschein and Hyatt [11], Lotz et al. [12,13], Carter et al. [14] and Ciarelli et al. [15].

$$r_{can} = \frac{(3.5362 \times Ecan) + 0.16128}{5} \quad \text{(1)}$$

$$r_{cor} = \frac{(0.2543 \times Ecor) + 3.09}{3} \quad \text{(2)}$$

The cortical thickness (*Tcor*) is another parameter to be evaluated. Previous studies by Mellal et al. [16] assumed a thickness of 1mm while Natali et al. [17] assumed 0.8 and 1.9mm. In the present study a more extensive range of *Tcor*, viz 0.3, 0.6, 0.9, 1.2, 1.5, 1.8 and 2.1mm is selected, see Figure 1. The Poisson's ratios, *v*, for the implant (grade 4 commercially pure titanium), cancellous and cortical bone are 0.3, 0.3 and 0.35 respectively. Note also that the cortical bone is constrained along the left and right faces of the cross-section in the distal direction (see Figure 1) thus representing a realistic function of the mandible with an implant.

3.2 Implant and loading

The dimensions of the Neoss [18] implant system are employed for the purpose of this study. Various dimensions are considered including lengths of 7, 9, 11, 13 and 15mm, and diameters of 3.5, 4.0, 4.5 and 5.5mm. This study only focuses on the stresses within the cancellous and cortical bone therefore the entire implant system has been simplified to being solely the implant, excluding the abutment, abutment screw and crown. In reality, the masticatory force is acting on the top of the crown. Neglecting the implant components above the implant itself means that the masticatory force is transferred to the head of the implant. This requires the introduction of a moment about the z-axis along with the forces acting in the vertical (*y*-axis), *Fv*, and horizontal (*x*-axis), F_H, directions.

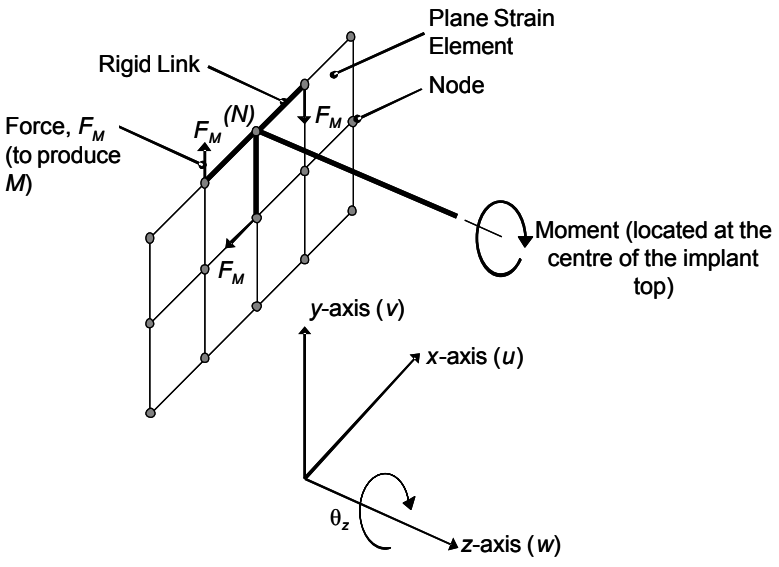

Figure 3: Moment applied to plane strain element

The F_H, F_V and M of 2 5 to 250N, 50 to 500N and 162.5 to 1625Nmm respectively are applied to the head of the implant, as shown in Figure 1, to simulate the masticatory forces. Note that M is applied in the negative z-axis and is based on the horizontal load laterally transferred at a distance (crown height) of 6.5mm. Based on the clinical study by Aparicio and Orozco [19], these loading conditions are considered comprehensive. In this study, $F_H/F_V/M$ combinations are chosen from the minimum values 25N/50N/162 .5Nmm to the maximum values 250 N/500N/1625Nmm together with half maximum values 125N/250N/812.5Nmm. Such a load combination and increment are used for all the parametric studies.

Due to the z-axis not being considered for the 2D plane strain elements, a moment must be applied through the use of rigid links to nodal points surrounding a specified node (N) at which the moment is applied (refer to Figure 3). At the end points of each rigid link, an orthogonal force F_M is applied thus creating a moment around the connecting point (N) of the rigid links.

4 Assumptions

In addition to assuming a 2D representation of the bone and implant, other assumptions are: (a) 50% osseointegration between the bone and implant; ,(b) linear relationships exist between the stress value and Young's moduli of the cancellous and cortical bone at any specific point.

4.1 Bone implant interface

The interface surrounding the implant exhibits both blood and bone fragments. This interface is considered clinically ideal for osseointegration. However it is mechanically unfavourable. The stage after insertion and before full osseointegration occurs is critical for the surrounding bone because it exhibits the most distinct stress concentrations. However post osseointegration, when the lamina dura is formed, the implant stability drastically increases.

In a finite element study by Natali et al. [17] two formation stages of the lamina dura were modelled by having Young's moduli of 0.3 and 1.5GPa, respectively. The formation of lamina dura improved the stress distribution more than cancellous bone and is a clinically favourable course of healing. A study by Berglundh et al. [20] assumed that the blood interface extended 0.13mm into the thread chamber. Based on these findings the present study assumes a 50% osseointegration between the bone and implant. The voids between the bone and implant are modelled as blood, see Figure 4. The Young's modulus and Poisson's ratio of the blood are taken as 0.7GPa and 0.3 respectively.

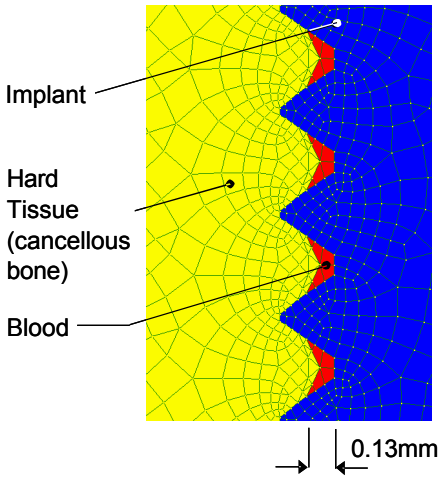

Figure 4: Proposed modelling of blood and hard tissue

4.2 Linear relationship between stress and Young's modulus

The possible number of parameter combinations for the bone, implant and loading exceeds 82,320. This number is based on five implant lengths, four implant diameters, fourteen Young's moduli each for cancellous and cortical bone, seven cortical thicknesses and three loading conditions (see Figure 1). It would be unviable to complete such a huge number of simulations. As a result, further assumptions are made to reduce the number of simulations hence yielding a manageable amount of data for analysis.

4.2.1 Predicted and actual stresses for Ecan and Ecor

The feasibility of a linear relationship for the stress variation for all combinations of *Ecan* and *Ecor* is exploited. In Figure 5 a methodology for predicting the linear relationship between the stress and the Young's modulus is shown. The actual stress values at any specific point along either VV or HH are recorded at the four corners representing the combinations of the minimum and maximum values of *Ecan*

and *Ecor*. Between any two actual stress values where either *Ecan* or *Ecor* is constant, a linear relationship between the stress and *Ecan* (or *Ecor*) is predicted. This prediction is then extended to any combination of *Ecan* and *Ecor*, provided that one of them remains constant.

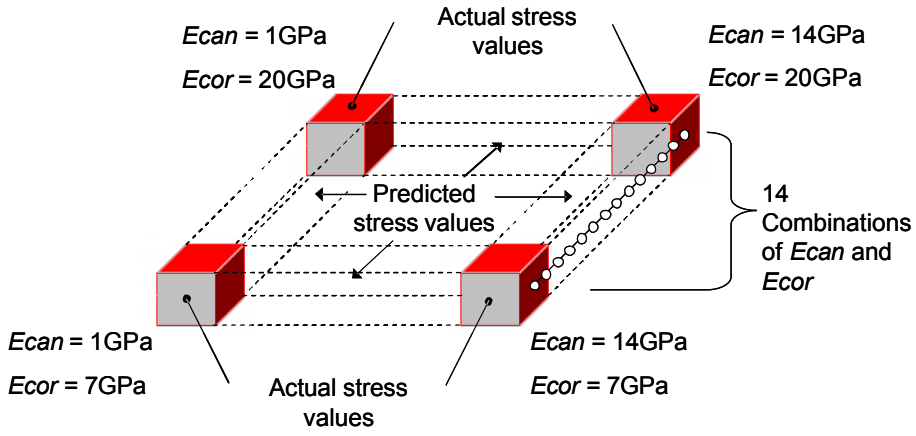

Figure 5: Methodology for predicting the linear relationship

For the purpose of validation, a finite element analysis is carried out to obtain the actual von Mises stress values for L = 11 mm, D = 4.5mm, $Tcor$ = 1.2mm, F_V = 500N, F_H = 250N and M = 1625Nmm. Varying *Ecan* from 1 to 14GPa for every possible value of *Ecor* shows little variation from linearity [9]. The actual stress at mid-point of line VV is recorded for all combinations of *Ecan* and *Ecor* and compared to the respective linear prediction. For *Ecan* = 7GPa and *Ecor* = 13GPa, the predicted stresses vary from the actual ones by an average of 5.7% and 4.3% respectively. The stresses recorded at mid-point of line HH produced similar percentage errors (4.9% and 6.5% for *Ecan* and *Ecor* respectively) to VV.

4.2.2 Parameter combinations

With the assumption of linear relationships between the stress and *Ecan* or *Ecor*, only the minimum and maximum values of Young's modulus are considered for each type of bone instead of the initial data set of fourteen. Parameters summarised in Figure 6 are thus evaluated. This means that the total number of analyses is reduced to 1680.

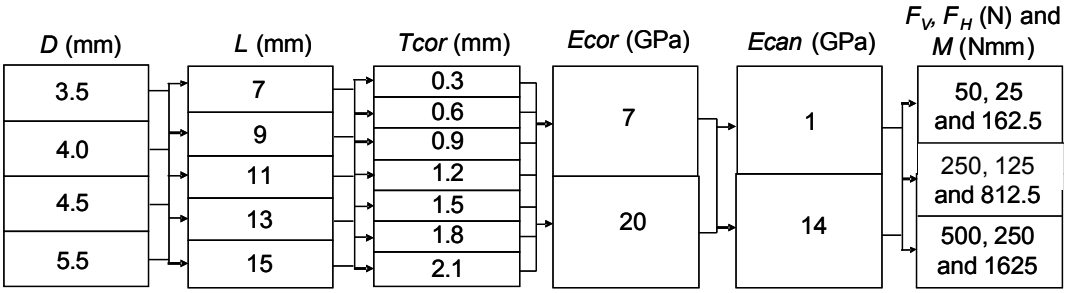

Figure 6: Parameter combinations

5 Discussion and Conclusion

This paper presents the methodology and analysis techniques that are used in the companion paper (Part II) to evaluate the stress distribution characteristics in the bone due to the effect of various parameters. Realistic geometries, material properties, loading and support conditions for the jawbone and implant are taken into consideration. Modelling assumptions in terms of (a) 50% osseointegration between bone and implant; (b) linear relationships between the stress value and the Young's moduli of the cancellous and cortical bone at any specific point, are discussed in some detail in this paper.

The parametric analysis covering the influence of varying each parameter on the stress characteristics in the mandible is presented in the companion paper (Part II).

6 References

[1] Branemark PI, Adell R, Breine U, Hansson BO, Lindstrom J, Ohlsson A. Intra-osseous anchorage of dental prostheses. I. Experimental studies. Scand J Plast Reconstr Surg. 1969;3(2):81-100.

[2] Branemark PI, Hansson BO, Adell R, Breine U, Lindstrom J, Hallen O, Ohman A. Osseointegrated implants in the treatment of the edentulous jaw. Experience from a 10-year period. Scand J Plast Reconstr Surg. 1977;16:1-132.

[3] Mellal A, Wiskott HW, Botsis J, Scherrer SS, Belser UC. Stimulating effect of implant loading on surrounding bone. Comparison of three numerical models and validation by in vivo data. Clin Oral Implants Res. 2004;15(2):239-248.

[4] Carter DR, Orr TE, Fyhrie DP, Schurman DJ. Influences of mechanical stress on prenatal and postnatal skeletal development. Clin Orthop Relat Res. 1987;(219):237-250.

[5] Himmlova L, Dostalova T, Kacovsky A, Konvickova S. Influence of implant length and diameter on stress distribution: a finite element analysis. J Prosthet Dent. 2004;91(1):20-25.

[6] Plikçiolu H, Akça K. Comparative evaluation of the effect of diameter, length and number of implants supporting three-unit fixed partial prostheses on stress distribution in the bone. J Dent. 2002;30(1):41-46.

[7] Pierrisnard L, Renouard F, Renault P, Barquins M. Influence of implant length and bicortical anchorage on implant stress distribution. Clin Implant Dent Relat Res. 2003;5(4):254-262.

[8] Strand7 Pty Ltd (2004), Strand7 Theoretical Manual, Sydney, Australia.

[9] van Staden RC, Guan H, Loo YC. Johnson NW, Ivanovski S, Meredith N. Influence of Bone and Dental Implant Parameters on Stress Distribution in Mandible – A Finite Element Study. *Int J Oral Maxillofac Implants.* (Submitted).

[10] van Staden RC, Guan H, Loo YC. Application of the finite element method in dental implant research. Comput Methods Biomech Biomed Engin. 2006;9(4):257-270.

[11] Abendschein W, Hyatt GW. Ultrasonics and selected physical properties of bone. Clin Orthop Relat Res. 1970;69:294-301.

[12] Lotz JC, Gerhart TN, Hayes WC. Mechanical properties of trabecular bone from the proximal femur: a quantitative CT study. J Comput Assist Tomogr. 1990;14(1):107-114.

[13] Lotz JC, Gerhart TN, Hayes WC. Mechanical properties of metaphyseal bone in the proximal femur. J Biomech. 1991;24(5):317-329.

[14] Carter DR, Schwab GH, Spengler DM. Tensile fracture of cancellous bone. Acta Orthop Scand. 1980;51(5):733-741.

[15] Ciarelli MJ, Goldstein SA, Kuhn JL, Cody DD, Brown MB. Evaluation of orthogonal mechanical properties and density of human trabecular bone from the major metaphyseal regions with materials testing and computed tomography. J Orthop Res. 1991;9(5):674-682.

[16] Mellal A, Wiskott HW, Botsis J, Scherrer SS, Belser UC. Stimulating effect of implant loading on surrounding bone. Comparison of three numerical models and validation by in vivo data. Clin Oral Implants Res. 2004;15(2):239-248.

[17] Natali AN, Pavan PG, Ruggero AL. Analysis of bone-implant interaction phenomena by using a numerical approach. Clin Oral Implants Res. 2006;17(1):67-74.

[18] Neoss Limited (2006), Neoss Implant System Surgical Guidelines, UK.

[19] Aparicio C, Orozco P. Use of 5-mm-diameter implants: Periotest values related to a clinical and radiographic evaluation. Clin Oral Implants Res. 1998;9(6):398-406.

[20] Berglundh T, Abrahamsson I, Lang NP, Lindhe J. De novo alveolar bone formation adjacent to endosseous implants. Clin Oral Implants Res. 2003;14(3):251-262.

Stress Distribution in Mandible Regulated by Bone and Dental Implant Parameters: Part II – Parametric Analysis

R. C. van Staden[1], H. Guan[1], Y. C. Loo[1], N. W. Johnson[2], N. Meredith[3]

[1]*Griffith School of Engineering, Griffith University Gold Coast Campus, Australia*

[2]*School of Dentistry and Oral Health, Griffith University Gold Coast Campus, Australia*

[3]*Neoss Ltd, Harrogate, United Kingdom*

Abstract: In this paper the finite element procedure is used to evaluate various bone, implant and loading parameters for their influence on the stress distribution within the bone, in particular in the mandible. The methodology and analysis techniques employed to enable accurate modelling of the implant and bone systems are discussed in the companion paper (Part I). The analysis results show that an increase in the Young's moduli for the cancellous and cortical bone yields elevated stress magnitudes in the bone. Thinner cortical bone results in elevated stress levels within itself as well as in the cancellous bone. In both cancellous and cortical bone, the implant length demonstrates to be more influential, in terms of differences between the minimum and maximum stress values, as compared to the diameter. The masticatory forces exhibit a more significant influence on the stress than all the other parameters. Therefore loading should be considered an imperative factor when planning an implant placement.

Keywords: bone, implant and loading parameters, finite element technique.

1 Introduction

The Finite Element Method (FEM) is becoming widely used to advance dental technologies [1,2]. The use of the FEM allows for an improved understanding of stresses within the implant and bone systems. Areas of application in dental implantology include studies on jawbone and implant properties as well as the bone implant interface [3-7]. Using the finite element technique the stress profile can be evaluated within both cancellous and cortical bone. This stress profile can be validated with the stress-strain behaviour of both cancellous and cortical as defined by Burstein et al. [8] and Currey [9]. To date no published research appears to have investigated the stress profile in the bone when various combinations of bone, implant and loading parameters are considered. The outcome of this study may help dental practitioners to identify the stimulus state of the bone - hence, they would be able to predict success or failure for all combinations of implant length and diameter with given cortical bone thickness, and material properties of cancellous and cortical bone, under a range of masticatory forces.

2 Parametric Analysis

As discussed in the companion paper (Part I), modelling and simulation of a total of 1680 parametric combinations are performed using the Strand7 Finite Element Analysis System [10]. The first subsection includes a summary of the von Mises stress profiles, recorded along the lines VV and HH for cancellous and cortical bone respectively, where average values are chosen for the remaining parameters except for the masticatory forces. The results due to three combinations of the masticatory forces are presented, viz the minimum values of 25N/50N/162.5Nmm, the maximum values of 250N/500N/1625Nmm and the median values of 125N/250N/812.5 Nmm. For example when presenting the stress for different values of *L*, the *Ecan, Ecor, D* and *Tcor* are all set to their mean values. Note that for this subsection, when F_V, F_H and *M* are varied all other parameters are set to their mean values. The second subsection summarises the most and least influential parameters where all the results presented correspond to the maximum masticatory forces.

2.1 Influence of varying each parameter

Figures 1 (a) and (b) present the von Mises stress recorded along the lines VV and HH for all the possible values of *D*. Other parameters are set to their average values: *L* = 11 mm, *Tcor* = 1.2 mm, *Ecan* = 7GPa and *Ecor* = 13GPa. When *D* increases the stress along the line VV oscillates more significantly following the thread profile (Figure 1 (a)). Such an increased oscillation is a result of reduced distance between the implant thread and cortical bone and the subsequent reduced volume of cancellous bone. This reduces the capacity of cancellous bone in distributing the stress more evenly. The stresses along the line HH exhibit a reduction when *D* is increased (Figure 1 (b)). This reduction is caused by the larger diameter implant supporting an increased portion of the load thereby reducing the stress in the cortical bone. Generally higher stresses are found at the implant neck for all values of *D*. Note that the stress levels along the lines VV and HH increase as F_H, F_V and *M* increase, which is evident in Figures 1 (a) and (b).

Varying diameter, *D*

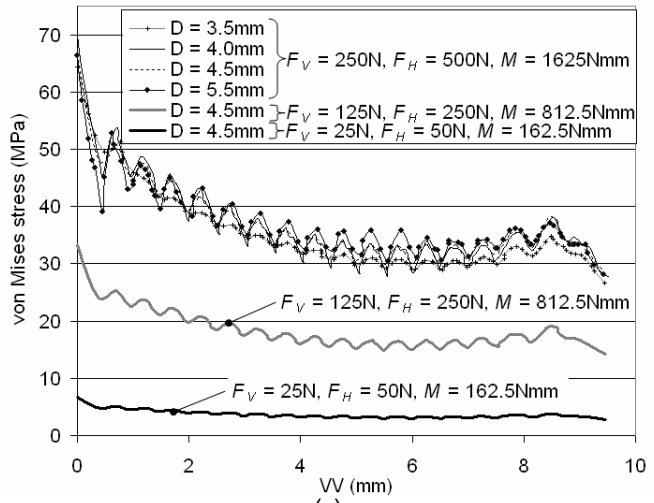

(a)

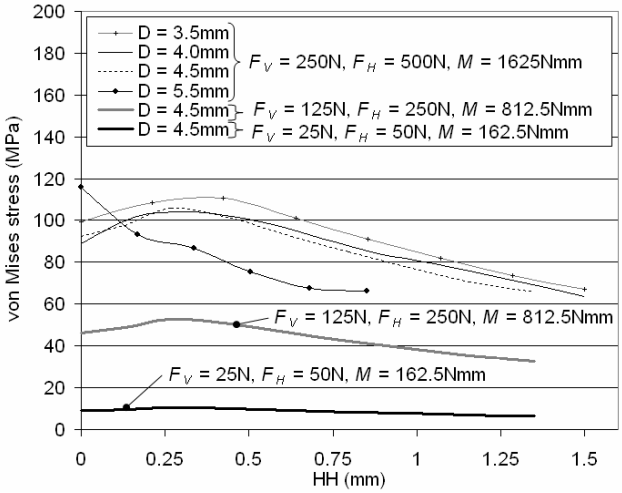

(b)

Varying length, *L*

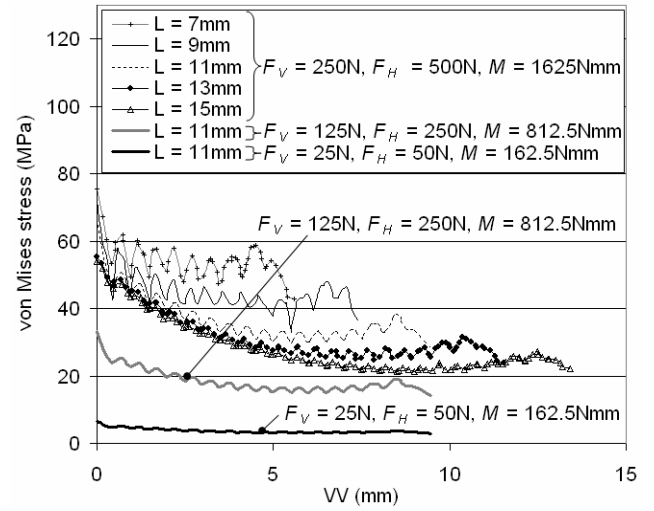

(c)

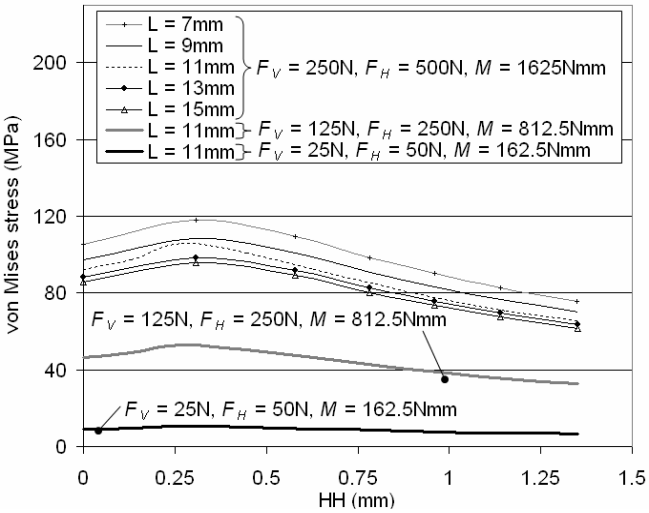

(d)

Varying cortical thickness, *Tcor*

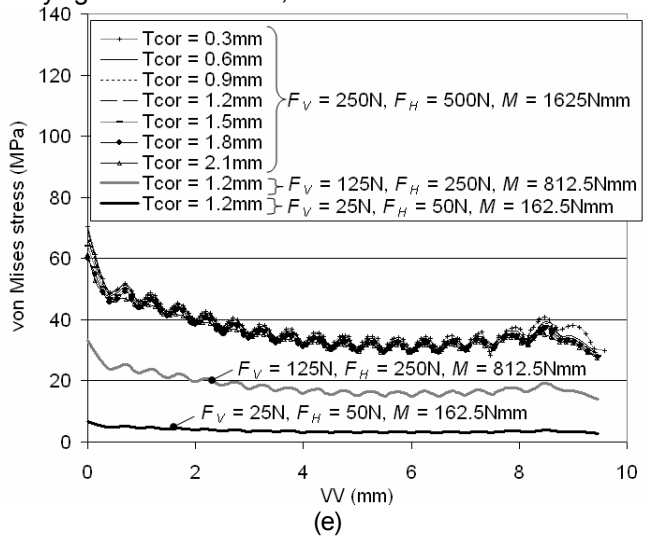

(e)

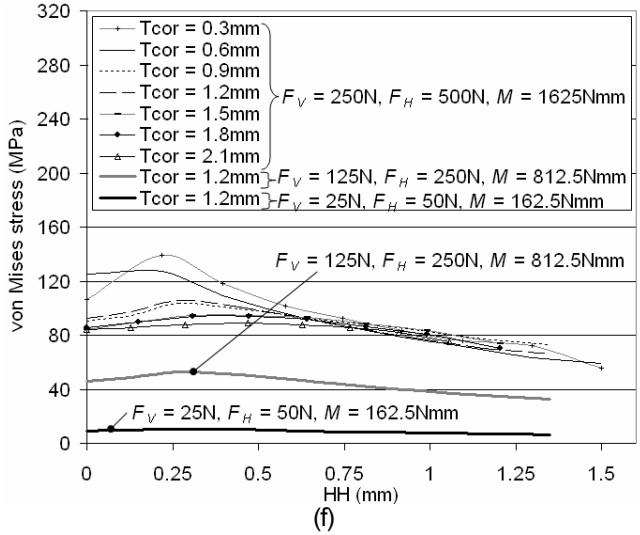

(f)

Varying Young's Modulus of cancellous bone, *Ecan*

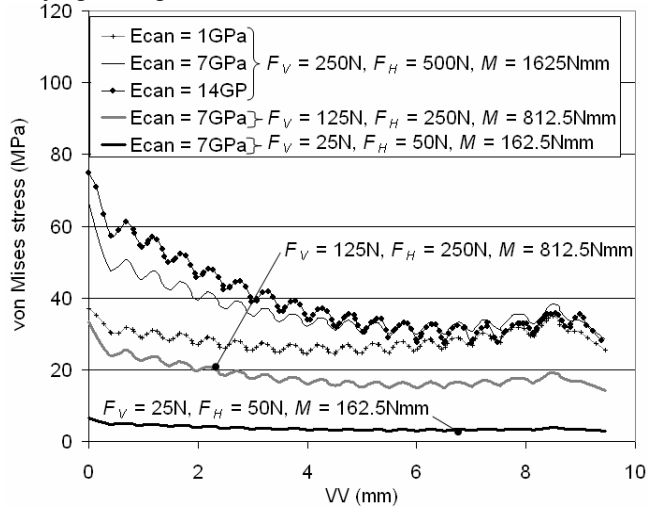

(g)

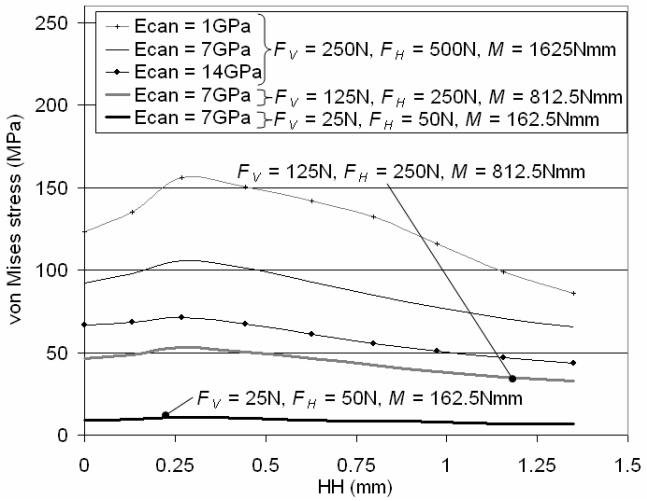

(h)

Varying Young's Modulus of cortical bone, *Ecor*

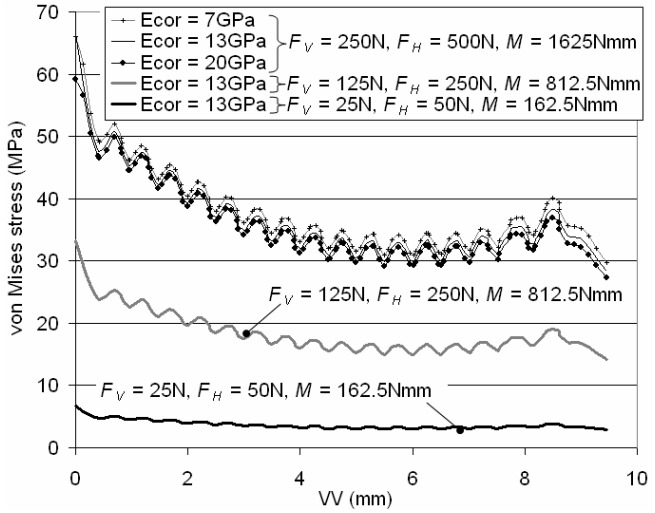

(i)

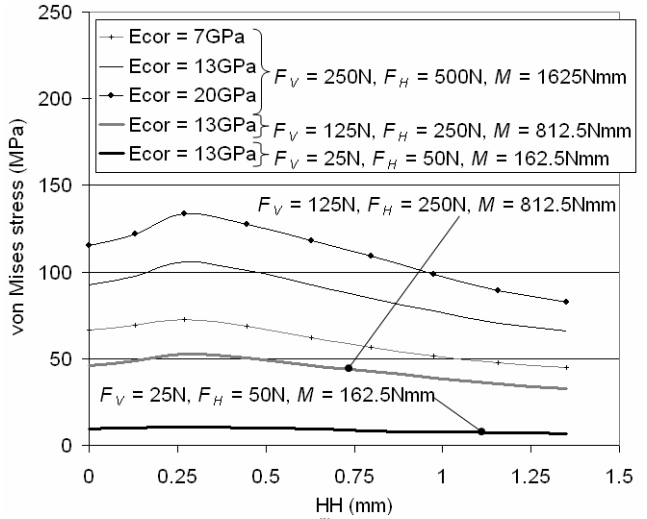

(j)

Figure 1: Stress profiles with varying parameters

The von Mises stress recorded along the lines VV and HH, for all possible implant lengths, are shown in Figures 1 (c) and (d). The stresses decrease within both cancellous and cortical bone (Figures 1 (c) and (d) respectively) as *L* increases because the surface area contact between the bone and implant also increases leading to the implant absorbing more load.

Figures 1 (e) and (f) present the von Mises stress recorded along the lines VV and HH for all possible values of *Tcor*. As *Tcor* decreases, the ability of the cortical bone in supporting the load also decreases leading to a slight increase in the magnitude of stresses along the line VV (Figure 1 (e)). No discernable trend is found for the stress profiles along the line HH, as shown in Figure 1 (f).

With reference to Figure 1 (g), as *Ecan* increases the stress magnitude increases. This is due to the cancellous being able to support a greater portion of the load. The stress within the cortical bone, Figure 1 (h), increases as *Ecan* decreases. This is because the cancellous bone is supporting less load and therefore an increased portion of the load has to be supported by the cortical bone.

As evident in Figure 1 (i), as *Ecor* decreases the stress magnitude increases slightly in the cancellous bone, which is due to the cancellous having to support an increased portion of the load. However the stress within the cortical bone, Figure 1 (j), increases as *Ecor* increases. This is due to the cortical bone having increased resistance to the load.

2.2 Parameter ranking

To identify the most and least influential parameters, all the six parameters given in Figure 6 of the companion paper (Part I) are ranked in this subsection. Based on the data shown in Figure 1, the average differences (*AD*) are analysed and discussed, where *AD* is defined as the difference between the stresses when a single parameter is set to its minimum and maximum values while all the other parameters are set to their mean values. The differences in stress at distances 1, 4.5, 9mm from V_1 and 0.2, 0.6, 1mm from H_1 along the lines VV and HH respectively (see Figure 1 of companion paper), are given in Table 1. However, for D = 3.5mm the differences in stress along the line HH are recorded at distances 0.2, 0.4 and 0.8mm from H_1. Note that *F-M* represents F_H, F_V and M by presenting the average stress difference that result from varying each load from minimum to maximum.

Table 1. von Mises stress (MPa) in cancellous and cortical bone (stress along the line HH shown in brackets)

VV/HH (mm)	*D*	*L*	*Tcor*	*Ecan*	*Ecor*	*F-M*
1 / 0.2	2.02, (16.86)	16.82, (21.92)	4.25, (53.29)	26.12, (66.80)	1.85, (52.98)	41.70, (87.80)
4.5 / 0.6	3.34, (25.70)	18.93, (18.19)	4.26, (16.24)	6.44, (81.33)	1.87, (55.80)	27.95, (83.27)
9 / 1	3.64, (22.27)	20.33, (15.17)	8.70, (3.06)	6.14, (52.02)	2.81, (41.58)	30.15, (69.66)
AD	3.00, (21.61)	18.69, (18.43)	5.74, (24.20)	12.90, (66.72)	2.18, (50.12)	33.27, (80.24)

When considering the *AD* in stresses along the line VV, the ranking order is *F-M>L>Ecan>Tcor>D>Ecor*. Where ">" indicates greater difference in stress than the next parameter. The applied loading (*F-M*) has a more significant influence on the stress differences than all other parameters. However, *Ecan* demonstrated differences in stress at the distance 1mm along the line VV that are closely matched by that of *L*. The Young's modulus of cortical bone (*Ecor*) exhibits the lowest *AD*, which is especially evident at a distance of 1 mm along the line VV. The ranking order for the *AD* in stress along the line HH is *F-M>Ecan>Ecor>Tcor>D>L*. As found for cancellous bone varying *F-M* has a major influence on the stress differences within the cortical bone. Varying *Tcor*, especially at 0.6mm along the line HH, has the least influence on the differences.

3 Stress Validation

Very similar to Currey's experimental results [9], the uniaxial compressive stress values for the human femora and tibiae measured by Burstein et al. [8] (Figure 2) are used as a reference to determine which parameters lead to either cancellous or cortical bone fracturing. Note also in this study that the compressive stresses on the right side of the implant are obtained under biaxial stress condition. Therefore a discrepancy is expected when the present results are compared to the uniaxial compressive stresses obtained by Burstein et al. [8].

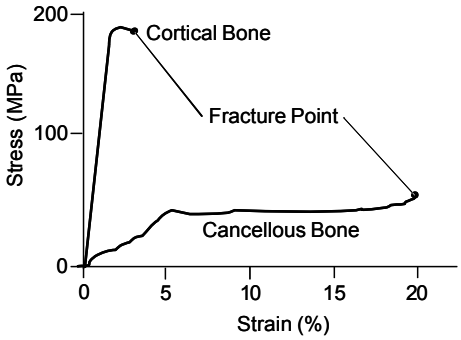

Figure 2: Stress-strain behaviour (Burstein et al. [10])

Derived from the stress-strain curve at the fracturing point are the uniaxial compressive stresses of 40MPa and 190MPa, for the cancellous and cortical bone respectively. Shown in Table 2 are the absolute maximum biaxial compressive stresses recorded along the lines VV and HH that are found close to the implant neck. Figure 3 presents the compressive stress profiles within the cancellous and cortical bone. Note that, for the data shown in Table 2 and Figure 3, all other parameters are set to their average values, with maximum loading combinations ($F_H/F_V/M$ = 250N/500N/1625Nmm).

Table 2. Absolute maximum compressive stresses (MPa) in cancellous and cortical bone

Parameter	*D* (mm)		*L* (mm)		*Tcor* (GPa)		*Ecan* (GPa)		*Ecor* (GPa)	
Line	3.5	5.5	7	15	0.3	2.1	1	14	7	20
VV	75.51	57.81	62.23	63.70	64.34	64.78	28.15	82.80	73.50	58.60
HH	133.63	113.25	145.80	111.06	164.24	106.69	163.55	90.04	92.48	157.94

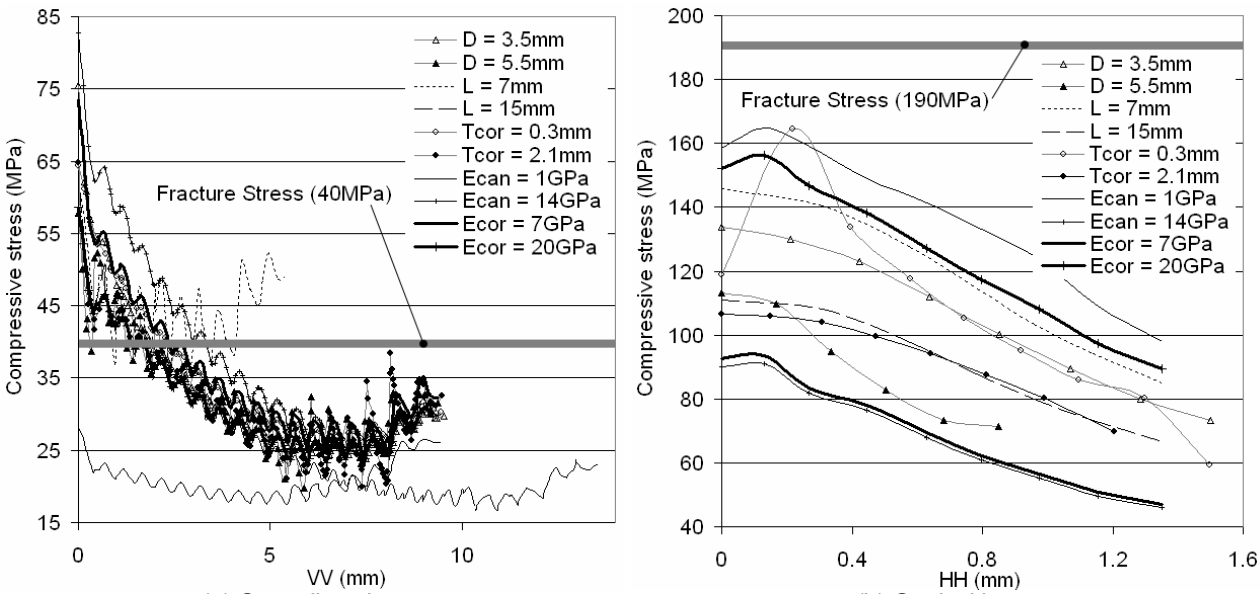

(a) Cancellous bone (b) Cortical bone

Figure 3: Absolute maximum compressive stress profiles in cancellous and cortical bone

For the majority of parameters the fracture stress of cancellous bone (40MPa) is exceeded (refer to Figures 3 (a) and (b)) close to the implant head along the line VV, with *D* exhibiting the highest stress out of all the parameters considered (refer to Table 2). However, the fracture stress for cortical bone is not exceeded for any of the parameters. O'Mahony et al. [6] found that the greatest compressive stresses in the cancellous and cortical bone were 20 and 115MPa respectively. Discrepancies between the results from the present study and those of O'Mahony et al. could be due to the different assumptions adopted for loading, modelling and restraint conditions: they assumed a 6 mm off-axial vertical load of 490N. On the other hand, the current study assumes F_H, F_V and M of 250N, 500N and 1625Nmm, respectively. Also O'Mahony et al. used an implant with no thread and they applied fixed constraints to the base of a two dimensional mandible section.

4 Discussion and Conclusion

A good agreement is found with previous research [11-17] which stated that an increase in implant length and diameter leads to a reduction in stress magnitudes within the cancellous bone. Note in this study however, when *D* increases the stress along the line VV oscillates more significantly following the thread profile (Figure 1 (a)).

A statement by Himmlova et al. [18] and Tawil et al. [16] indicates that the implant diameter (*D*) is more important for improved stress distribution than the implant length (*L*). However, it is shown herein that an increase in length reduces the stress, within both the cancellous and cortical bone, for a wider range of parameters. This is more obvious than the influence of varying diameter. In contrast, Pierrisnard et al. [12] found that the stress within the bone was virtually constant, independent of implant length and bicortical anchorage.

No research to date has considered the influence that the cortical thickness (*Tcor*) has on the stress in the cancellous and cortical bone. In this study it is concluded that decreased *Tcor* leads to cortical bone supporting less load leading to a slight increase in the magnitude of stresses in the cancellous bone. Generally, as the strength of either cancellous (*Ecan*) or cortical (*Ecor*) bone increases, their ability to carry the load increases. This is evident when considering the stress along the line VV, as when *Ecan* increases the stress magnitude increases, which is due to the cancellous being able to support more load. In addition and as expected, when decreasing *Ecor* the stress magnitude increases within the cancellous bone, which is due to the cancellous having to support a greater portion of the load. The stress within the cortical bone increases as *Ecor* increases, which is due to the cortical bone offering more resistance to the load.

It is found common during this study that elevated stress levels occur at the implant neck for all the parameter combinations. This phenomenon is supported by the study of Meijer et al. [5] which concluded that the regions of bone exposed to maximum stress are located around the implant neck. Note that the present study also found

that the stress level at the implant neck, within the cancellous bone, is influenced by the fact that elevated stress magnitudes are transferred through its contact with the cortical bone.

In general, the implant length has a noteworthy characteristic relationship with the stress in the bone. The length is more influential, in terms of the stress difference in the cancellous bone, than the diameter. However the diameters is more influential in the stress difference in the cortical bone. Overall, in both cancellous and cortical bone the applied load and moment are most influential and therefore it is considered an imperative factor when planning an implant placement.

When comparing the absolute maximum compressive stress values within both cancellous and cortical bone with published stress-strain data it is found that the cancellous bone experiences fracturing for all parameter combinations when maximum loading is applied. However, this is not the case when the loading is set to a magnitude that is half of the maximum. For the cortical bone the fracture point is never reached for all parameter combinations even when subjected to maximum loading. It is anticipated that these new findings will assist the clinician to perform a patient specific implant treatment in a more quality-controlled manner. Evaluating the influence of other parameters which affect the stress characteristics that govern osseointegration and bone growth, may constitute the main aim of a future study. These parameters include implant taperage, pitch and design of implant thread, implant neck offset, different percentages of osseointegration and implant orientation within the bone.

Acknowledgements

A special thank you goes to John Divitini and Fredrik Engman from Neoss Limited for their technical advice.

5 References

[21] DeTolla DH, Andreana S, Patra A, Buhite, R, Comella B. Role of the finite element model in dental implants. J Oral Implantol. 2000;26(2):77-81.
[22] Geng JP, Ma QS, Xu W, Tan KB, Liu GR. Finite element analysis of four thread-form configurations in a stepped screw implant. J Oral Rehabil. 2004;31(3):233-239.
[23] Menicucci G, Mossolov A, Mozzati M, Lorenzetti M, Preti G. Tooth-implant connection: some biomechanical aspects based on finite element analyses. Clin Oral Implants Res. 2002;13(3):334-341.
[24] Canay S, Hersek N, Akpinar I, Asik Z. Comparison of stress distribution around vertical and angled implants with finite-element analysis. Quintessence Int. 1996;27(9):591-598.
[25] Meijer HJ, Starmans FJ, Steen WH, Bosman F. Loading conditions of endosseous implants in an edentulous human mandible: a three-dimensional, finite-element study. J Oral Rehabil. 1996;23:757-763.
[26] O'Mahony A, Bowles Q, Woolsey G, Robinson SJ, Spencer P. Stress distribution in the single-unit osseointegrated dental implant: finite element analyses of axial and off-axial loading. Implant Dent. 2000;9(3):207-218.
[27] Patra AK, DePaolo JM, D'Souza KS, DeTolla D, Meenaghan MA. Guidelines for analysis and redesign of dental implants. Implant Dent. 1998;7(4):355-368.
[28] Burstein AH, Reilly DT, Martens M. Aging of bone tissue: mechanical properties. J Bone Joint Surg Am. 1976;58(1):82-86.
[29] Currey JD. The Mechanical Adaptation of Bones. New Jersey: Princeton University Press; 1984:3-36.
[30] Strand7 Pty Ltd (2004), Strand7 Theoretical Manual, Sydney, Australia.
[31] Plikçiolu H, Akça K. Comparative evaluation of the effect of diameter, length and number of implants supporting three-unit fixed partial prostheses on stress distribution in the bone. J Dent. 2002;30(1):41-46.
[32] Pierrisnard L, Renouard F, Renault P, Barquins M. Influence of implant length and bicortical anchorage on implant stress distribution. Clin Implant Dent Relat Res. 2003;5(4):254-262.
[33] Aparicio C, Orozco P. Use of 5-mm-diameter implants: Periotest values related to a clinical and radiographic evaluation. Clin Oral Implants Res. 1998;9(6):398-406.
[34] Iplikcioglu H, Akca K. Comparative evaluation of the effect of diameter, length and number of implants supporting three-unit fixed partial prostheses on stress distribution in the bone. J Dent. 2002;30(1):41-46.
[35] Misch CE. Implant design considerations for the posterior regions of the mouth. Implant Dent. 1999;8(4):376-386.
[36] Tawil G, Aboujaoude N, Younan R. Influence of prosthetic parameters on the survival and complication rates of short implants. Int J Oral Maxillofac Implants. 2006;21(2):275-282.
[37] Zhang L, Zhou Y, Meng W. A three-dimensional finite element analysis of the correlation between lengths and diameters of the implants of fixed bridges with proper stress distribution. Hua Xi Kou Qiang Yi Xue Za Zhi. 2000;18(4):229-231.
[38] Himmlova L, Dostalova T, Kacovsky A, Konvickova S. Influence of implant length and diameter on stress distribution: a finite element analysis. J Prosthet Dent. 2004;91(1):20-25.